Stochastic Treatment of Bump Latency and Temporal Overlapping in *Limulus* Ventral Photoreceptors

R. Lederhofer, J. Schnakenberg
Institut für Theoretische Physik, RWTH Aachen, Bundesrepublik Deutschland

H. Stieve
Institut für Biologie II, RWTH Aachen, Bundesrepublik Deutschland

Z. Naturforsch. **46c**, 291–304 (1991); received September 4, 1990

Quantum Bumps, Latency, First-Passage Time, Light-Evoked and Spontaneous Bumps, Poisson Statistics of Photons

We present quantum bumps obtained from flash experiments at the *Limulus* ventral nerve photoreceptor under voltage clamp conditions. The results are shown and discussed in form of histograms for the latency, amplitude and net charge transfer (current time integral) of the bump current responses. We argue that the experimental latency histograms cannot be described satisfactorily by chemical models if one assumes that not more than one photon is captured per flash. Instead of, one has to take into account the Poisson statistics of the captures of 0,1,2,... photons released by a single flash. We show that the inclusion of Poisson statistics makes the effective latency histograms of flash responses typically asymmetric and skewed towards short latencies as compared to that of model histograms for one-photon responses. Our conjecture also implies that under our experimental conditions a fraction of up to 20% of the bump responses evoked by a flash should be suspected to be superpositions of two ore more one-photon responses which cannot be separated by any kind of evaluation analysis. Consequently, the average values of amplitudes and net charge transfers of the light-evoked bump responses are expected to be overestimated as compared to that of true one-photon responses. This hypothesis is confirmed by a numerical simulation of light-evoked bump responses using experimentally recorded spontaneous bumps (at times larger than 1 s after the flash) as the simulation material. We show that the superposition of one-photon events in the light-evoked bump responses due to Poisson statistics settles the question why their amplitudes and net charge transfers are found to be larger than that of the spontaneous bumps. We suggest that true one-photon responses evoked by a light flash and spontaneous bumps start from the same activated rhodopsin state and take the same biochemical pathway.

1. Introduction

Many photoreceptor cells of invertebrates show so-called quantum bump responses if they are stimulated either by continuous light or by light flashes of sufficiently low intensity. Quantum bumps are transient responses of the recorded membrane potential or of the transmembrane current recorded under voltage clamp. A number of arguments have been given in the literature that quantum bumps are responses to the capture of a single photon by a rhodopsin molecule in the rhabdomal part of the membrane. In experiments with continuous light stimulus, bumps appear as a series of transient responses with a frequency proportional to the light intensity. In flash experiments at a fixed low intensity of the flash, one observes a fluctuating number of single bumps including cases without any response above the base line noise and also cases where different bump responses more or less overlap as functions of time.

In this paper, we report on bump experiments at the *Limulus* ventral nerve photoreceptor (VNP) and on a number of conclusions which we draw from our observations. Typical current bumps evoked by light flashes and recorded under voltage clamp are shown in Fig. 1. Bumps in the *Limulus* VNP vary quite largely with respect to their parameters amplitude, net charge transfer (time integral of bump current), duration and latency. Our particular interest in this paper will be focussed on latency. Latency is defined as the time elapsing between the evoking light flash and the first onset of the response signal above the base line noise. As compared to other photoreceptor cells, latencies in *Limulus* VNP are relatively large (mean value about 200 ms in the dark-adapted state at T =

Reprint requests to Prof. Dr. H. Stieve.

Verlag der Zeitschrift für Naturforschung, D-7400 Tübingen
0939–5075/91/0300–0291 $ 01.30/0

15 °C). The histogram of latencies obtained from a number of flash responses (between 200 and 300 flashes, *cf.* Fig. 2) shows a characteristic shape: only very few bumps have latencies below 150 ms whereas the decay of the histogram towards larger latencies is much less pronounced. The fact that the histogram has a width of the same order as its mean value indicates that only a very small number of molecules are involved in the molecular process which determines the latency phenomenon. On the other hand, the bump process in *Limulus* VNP necessarily involves a high degree of amplification: from the experimental data a number of between 1000 and 10,000 transient channel opening events can be estimated for a single bump [1]. It seems very likely the latency and amplification are due to separated molecular mechanisms and that latency precedes amplification. One of us [2] has presented a comprehensive argumentation in favour of this hypothesis which will be taken as the basis of the analysis to be given in this paper. This consideration also implies that the transduction model suggested by Fuortes and Hodgkin [3] is inadequate for *Limulus* VNP since it describes latency and amplification as integrated mechanisms. The situation seems to be quite different for bumps in vertebrate photoreceptors where the latencies are much shorter and scatter much less as compared to *Limulus* VNP.

If the intensity of the evoking light flash is increased, the number of bumps also increases and moreover the bumps tend to overlap as functions of time and thus eventually summarize to a macroscopic response. Experimentally, one observes that the latency decreases with increasing intensity down to about 30 ms for high intensities [1]. If one assumes that the bumps contained in a macroscopic response are independent events the latency of the macroscopic response can be interpreted as the shortest among the latencies of a large number of bumps. It is clear that with increasing number of bumps the shortest latency decreases. This seems to us the most plausible explanation why the latency of macroscopic responses decreases with increasing flash intensity. One of us [4] has worked out this idea and found an almost quantitative agreement with the experimental behaviour of latency. Payne and Fein [5] observed for *Limulus* VNP that latency also depends slightly on the spatial density of photon captures on the membrane. This finding would indicate that the bumps contained in a macroscopic response are not independent, at least for high flash intensities. For the purpose of this paper, we need not take into account this possibility since we restrict ourselves to rather low flash intensities (less than about 5 bumps per flash).

Our procedure in this paper starts with a presentation of our experimental methods and results in chapter 2 and 3. In chapter 4, we argue that latency in bump experiments cannot be described adequately by any kind of a model which starts from the capture of exactly one photon per flash. Our basic conjecture is that even for low intensities one has to take into account the finite probabilities for the capture of a number of $n = 0,1,2,\ldots$ photons per flash due to Poisson statistics of photons. In chapter 5, we show that inclusion of the Poisson statistics of photons makes the latency histogram typically skewed towards short latencies as observed in the experiments. This phenomenon is independent of any detailed transduction model for one-photon processes. In chapter 6, we suggest two such detailed models and discuss their particular fits to the experiments. Our conjecture has further implications which we did not expect at the beginning of our work. Due to the finite probability that more than one photon is captured per flash, one has to realize that the corresponding response consists of more than one single photon response as observed in the experiments (*cf.* Fig. 1). A crucial point, however, is that a fraction of those responses may overlap in time. If the overlap is almost complete, the corresponding response is misinterpreted as a single response and its amplitude and its net charge transfer are overestimated as compared to the that of true one-photon response. We suggest that this effect may explain why the so-called spontaneous bump responses recorded at times larger than about 1 s after the flash are found to be smaller in size. This suggestion is quantitatively worked out in chapter 7. Lamb [6] and Lisman [7] have conjectured that the spontaneous bumps are caused by spontaneous backward reactions of inactivated rhodopsin into an active configuration. In order to account for the different sizes of spontaneous bumps, Lisman assumed different transduction pathways for light-evoked and spontaneous bumps. In view of our arguments, this latter assumption is no longer

compelling: light-evoked and spontaneous bumps may start just as well from the same activated rhodopsin state and take the same transduction pathway.

2. Experimental Methods

Bumps were recorded in the ventral nerve photoreceptor cell of *Limulus* as membrane current signals under voltage clamp conditions. Two intracellular electrodes were used for the recording in a standard way [8]. During the experiment the ventral nerve was continuously superfused by physiological saline of constant temperature, 15 °C. Two types of light stimuli were adopted, both filtered through a broadband interference filter (540 ± 40 nm):

1. A very weak bump-evoking xenon flash of 50 μs duration administered through a 540 ± 40 nm interference filter every 10 s. It was adjusted in intensity by neutral density filters so as to evoke about 1–2 bumps recognizable within the first second after the flash and was kept constant throughout the entire experiment. Its energy E_e was in the order of 10^8 photons/cm^2.

2. A conditioning, light-adapting flash of 10 ms duration from a xenon lamp. Its energy E_c was about 100 times greater than E_e. In alternating periods of the experiment the conditioning flash was either applied 2 s prior to the constant bump evoking flash, or omitted.

The measured membrane current was digitized with a frequency of 1 kHz, stored on tape and later on processed and evaluated by a computer program. The noise level of the registrations varied from cell to cell between 20 and 100 pA. The accuracy of measurement was 20 pA and 1 ms.

Procedure

After impalement by the two microelectrodes the photoreceptor cell was dark-adapted for about 1 h.

In the following first period of the experiment only the bump-evoking flash was administered every 10 sec, for 50–250 times.

In the next period of the experiment the bump-evoking flash was again repeated every 10 s for 50–250 times, however, each time 2 sec prior to the bump-evoking flash the conditioning flash was administered. The conditioning flash was applied in order to study the effect of weak light adaptation by conditioning pre-illumination on the bump response evoked by the constant bump-evoking flash. The responses to the bump evoking stimuli were recorded for the following 8 s, measured individually, and the distribution of the bump parameters (see below) plotted.

Most bumps occurred within the first second after the bump-evoking flash. During the following 7 sec bumps were considerably less frequent (≤0.1/s, compared to 2.7/s during the first second).

The experiments (KL 98 and KL 99) lasted between 1 and 2 h.

Evaluation

Our computer program could detect bumps only if their amplitude was larger than 50–100 pA and their net charge transfer larger than 5 pC. We estimate that the lowest limit for the amplitude of the smallest possible bumps might be *ca.* 1 pA [9].

The program determined a number of bump parameters:

TLAT, latency: the time from the beginning of the stimulus to the first measurable deflection of the membrane current from the baseline, *i.e.* the time when the signal exceeds two times noise level.

TA, time-to-peak: the time from the beginning of the stimulus to the maximum of the bump.

TB, bump-width or bump duration: time from the end of the latency until the current has returned into the baseline noise.

A, amplitude of the bump maximum.

F, area: current-time-integral of the bump over TB.

We distinguished between these different types of bumps:

1. Apparently single bumps:

All parameters were determined. A certain percentage of these responses were probably mistaken for single bumps although they were superpositions of several totally overlapping bumps. See Fig. 1 A to D.

2. Apparently superimposed bumps:

– "Riders": bumps riding on top of a preceding bump; having their maximum after the maximum of the preceding bump. From riders only TA, the time-to-peak, was determined.

– "Horses": bumps having a rider on top after the maximum: latency, time-to peak and height of the maximum were determined. See Fig. 1 F, G, H.

(For more experimental details see [9–11].)

3. Experimental Results

If the dark-adapted photoreceptor of *Limulus* is stimulated by light flashes which are so weak that not every flash evokes a light response, one observes bumps, responses of the photoreceptor to the successful absorption of single photons (Fig. 1 A to E). A bump is a transient increase in the cation conductance of the visual cell membrane and follows photon absorption after a long, greatly variable delay (latency). The time course of the bump is temperature-dependent.

Bumps evoked under identical experimental conditions by photons of the same wave-length vary greatly in size, shape and latency (see Fig. 1, 2 A and 3). The average latency of bumps of a dark-adapted photoreceptor cell of *Limulus* (15 °C) is *ca.* 200 ms. The bump current rise lasts about 30 ms and the bump decline almost 60 ms.

The bumps were observed to be most frequent in the first second after the bump-evoking flash and became sparse in the following seconds. Bumps are observed even after stays for more than 1 h of the photoreceptor in the dark, they are called "spontaneous" bumps. The vast majority of the light-evoked bumps occurred within the first second after the flash whereas the later observed bumps were predominantly "spontaneous" bumps. However, this one second time limit is somewhat arbitrary.

To estimate the frequency of the "spontaneous" bumps we counted the bumps in the 6th, 7th and 8th second of the cycle to minimize the probability of contamination by light-evoked bumps. On the average the bump rate in this interval is about 0.1 bumps per second. If the spontaneous bump rate is not much altered by the bump-evoking flash there will be about the same rate of spontaneous bumps during the first second of the cycle. However, there is no way to decide for a single observed bump, whether it is a "spontaneous" or a light-evoked bump. The rate of "spontaneous" bumps is strongly temperature-dependent [12, 13].

This type of experiments is described in greater detail in [9].

A bump of a *dark-adapted* photoreceptor cell of *Limulus* is based on a sodium ion-preferring con-

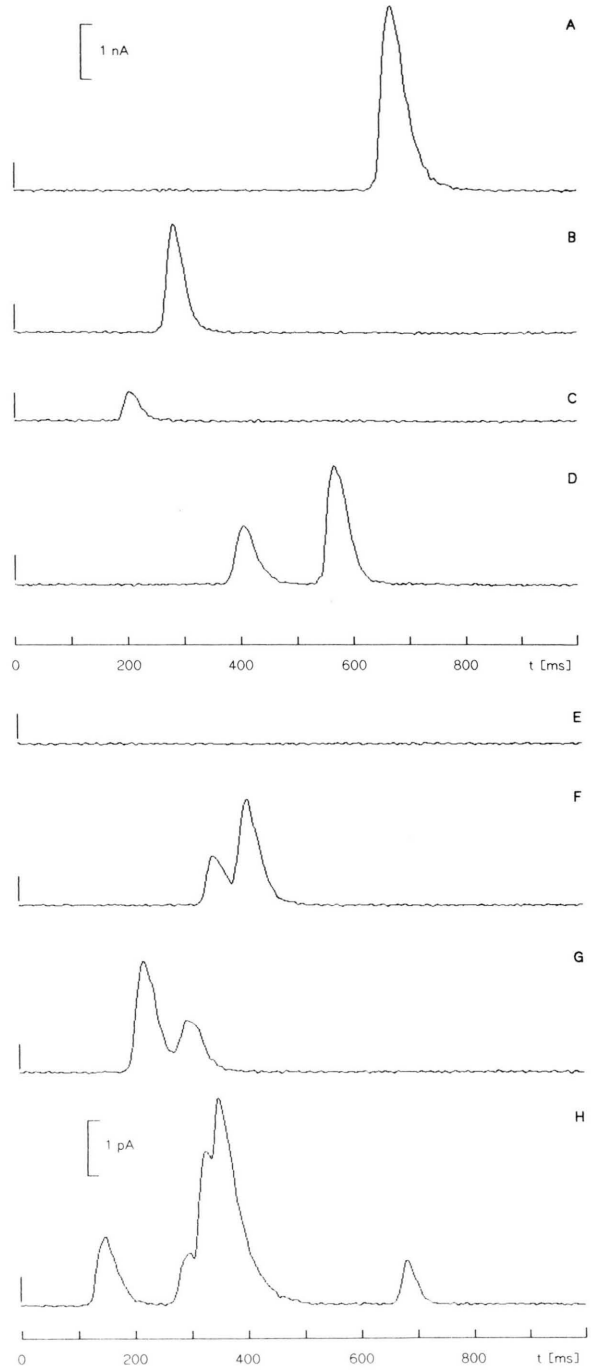

Fig. 1. Current response measured from a dark-adapted *Limulus* ventral nerve photoreceptor under voltage-clamp conditions (experiment KL 98). Inward currents are counted positive. Part A to D show typical bump responses, part F, G and H show bumps overlapping in time. Bump-evoking flash: $0.82 \cdot 10^8$ photons/cm^2, duration: 50 µs, wavelength: 540 nm, membrane potential clamped to −40 mV, 15 °C.

ductance increase of on the average about 5 nS in the maximum of the bump, occasionally up to 20 nS [14–17]. This leads to the estimate that at least 10^4 light-activated ion channels are simultaneously opened in the maximum of a large bump. Bump size and latency are not correlated; they vary independently from each other [11, 18–21]. Fig. 2 and 3 show the frequency distribution of bump latency, bump amplitude, and bump current time-integral.

The distributions are all asymmetrically bell-shaped (Fig. 2, 3). There may be a large number of bumps which are smaller than the noise level and thus escape our detection. If one plots the latency of all first bumps observed within the first second after the bump-evoking flash, one obtains a distribution as in Fig. 2A. The distribution of the latencies of all recognized bumps (*i.e.* including the latencies of the second, third ... *etc.* bump, if more than one bump occurs in the first second) observed within the first second is slightly different (Fig. 2B).

If one, however, plots the amplitudes of the bumps observed within the first second compared

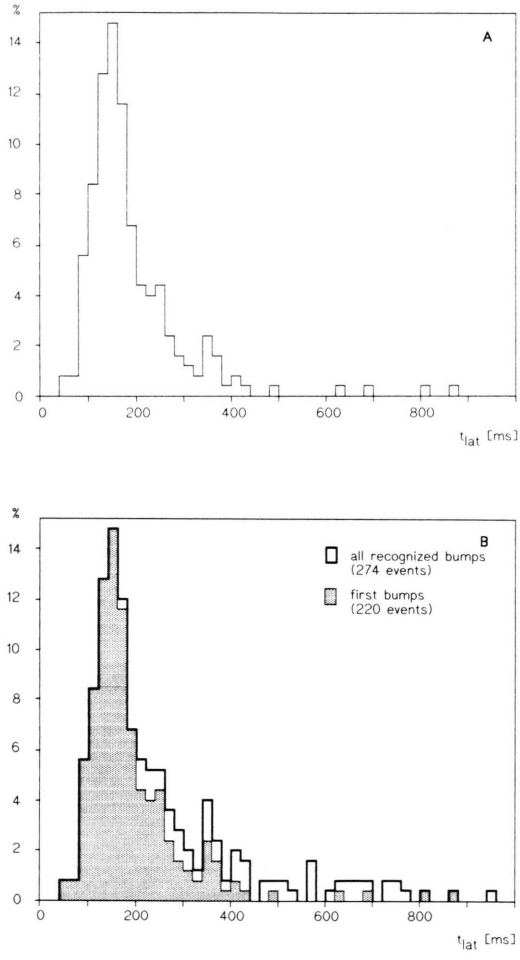

Fig. 2. Frequency distribution of bump latencies (experiment KL 98, dark-adapted cell). A: Only latencies of first bumps following the flash (220 events). B: Comparison of latencies of first bumps (hatched area, same as A) and latencies of all recognized bumps after the flash (274 events).

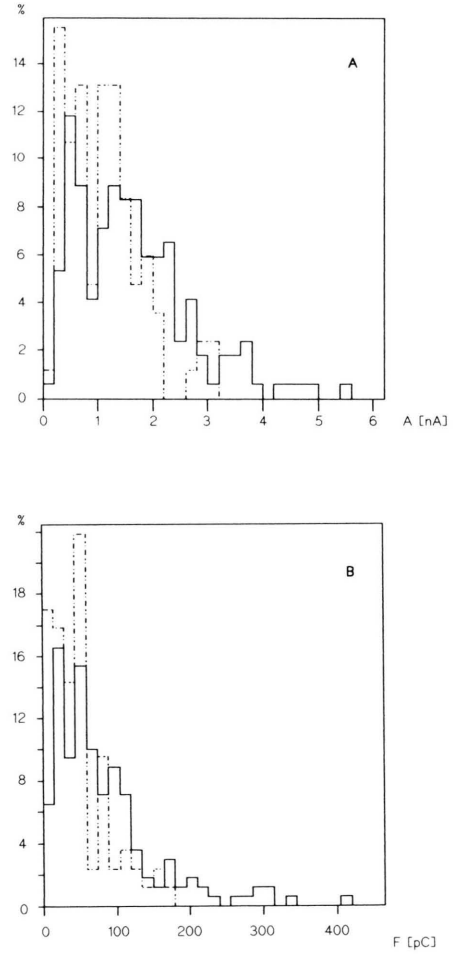

Fig. 3. Frequency distributions of bump amplitudes (A) and net charge transfer (B) from experiment KL 98. Full line: bumps with latency shorter than 1 s (169 events); broken line: bumps with latencies longer than 1 s (84 events).

to the amplitudes of the bumps after the first second, one sees that on the average the bumps within the first second are larger, but their frequency distributions of the bumps amplitudes overlap greatly. The same applies to the bump current time-integral (Fig. 3).

Later we will deal with the question whether these differences in size of the observed bumps are based on differences in the single photon-evoked events, or whether they are an experimental artefact based on our inability to discriminate between a single bump or an event composed of more than one totally overlapping bump if the overlap is close in time.

4. Latency Models

In the photoreceptor literature, transduction is commonly and quite suggestively modelled as a chain of chemical reaction steps [2, 3, 5, 22, 23]. In any of such models, the transduction chain is assumed to be initiated at its head end by the absorption of a photon by a rhodopsin molecule, and the final step at its tail end is assumed to be the opening (for invertebrates) or the closing (for vertebrates) of one or more ionic channels. For the case of the *Limulus* VNP, the model chain necessarily involves amplification as well as diffusion, since the capture of a single photon causes the transient opening of between 1000 and 10,000 ionic channels ("single photon bump") which are spread in a membrane region of about a few μm diameter ("bump speck") [1, 24].

In the scope of such models, latency is to be interpreted as the time t of the first channel opening or closing event after the chain was initiated at its head end at $t = 0$ by photoisomerization of a rhodopsin molecule. This time is usually referred to in the literature of stochastic processes as the so-called first-passage-time (fpt) [25]. The fpt of a model chain is a fluctuating quantity, *i.e.*, one obtains different values for the fpt's of different trials all started by the same initiation, namely a photon capture at $t = 0$. The reason for this fluctuation lies in the fact that the chains contain reaction steps with a very small number of particles involved, at least near their head ends, and that a chemical reaction is a stochastic process by its very nature. One of the main subjects of a stochastic investigation of a model chain is hence to calculate its fpt-density $\varrho(t)$ which is defined such that $\varrho(t)\mathrm{d}t$ is the probability to find a fpt in the time interval $(t, t + \mathrm{d}t)$. The larger the number of steps in the model chain, the smaller we expect the variance of $\varrho(t)$. This is a particular consequence of the central limit theorem, *cf.* Eqn. (4.2). In a first approach, one should then compare the calculated fpt-density $\varrho(t)$ with the latency histograms observed in bump experiments. As to be shown below, such a direct comparison delivers rather unsatisfying results for a very broad class of chain models at least in the case of *Limulus* VNP.

Before discussing particular properties of latency models for *Limulus* VNP, we have to recall a conclusion of a prior investigation of latency in *Limulus* VNP by one of us [2]. The first 4 to 8 steps of the chain following its initial step should be gainless, *i.e.*, not amplifying, and the latency is expected to be produced essentially by these first gainless steps. The main argument for this conclusion is that the ratio t_B/t_{lat} of the bump duration t_B and the mean latency time t_{lat} becomes quite unrealistic as compared to the experimental findings if amplification were assumed to set in from the very beginning of the chain. Note that the situation may be quite different in vertebrate photoreceptors where latency is much less pronounced and fluctuates very slightly. This indicates that the transduction chain in vertebrates presumably amplifies from the very beginning. For our case of the *Limulus* VNP, however, we now formulate a simple latency model as a series of a number N of gainless reaction steps with equal rate constants k:

$$\text{photon capture} \rightarrow X_0 \xrightarrow{k} X_1 \xrightarrow{k} \ldots \xrightarrow{k} X_N. \quad (4.1)$$

After a photon has been absorbed, the conformation X_0 of some molecule is formed which undergoes a series of N first-order reaction steps until finally the conformation X_N starts amplification which is not explicitly shown in the above scheme. The steps in the scheme (4.1) are obviously gainless. We assume that latency is exclusively caused by these gainless steps and that the latency period ends as soon as amplification is started. The fpt-density of the scheme (4.1) can be calculated analytically, the result being

$$\varrho(t) = k \frac{(kt)^N}{N!} \mathrm{e}^{-kt}, \text{ such that } \int_0^\infty \mathrm{d}t\varrho(t) = 1. \quad (4.2)$$

The model scheme in (4.1) can be realized chemically in many different ways. Another interpreta-

tion is that the photon-induced conformation X_0 is able to bind a number of N ligands step by step such that the final state X_N with N ligands bound to X_0 starts amplification. With this interpretation, the value of the ligand concentration enters into the rate constant k and has to be assumed absolutely constant and light-independent.

When trying to fit the above result for $\varrho(t)$ to the experimentally obtained histogram of latencies of the first bumps after the light flash, we first observe that the rate constant k is determined by the time scale: $\varrho(t)$ of (4.1) has a maximum at $t_m = N/k$ which is chosen equal to the maximum of the experimental histogram, *i.e.* $t_m \approx 200$ ms. This fixes k if N is given. Thus N remains the only parameter to be fitted. The best fit is obtained for $N \approx 8$ as shown in Fig. 4.

The quality of the fit is rather poor: the model fpt-density $\varrho(t)$ is too broad as compared to the experimental histogram. Choosing a larger value of N would make $\varrho(t)$ narrower but also more symmetric around its maximum at t_m (for large N $\varrho(t)$ tends to a completely symmetric Gaussian density). In contrast, the experimental histogram is markedly asymmetric: only a very few bumps have latencies shorter than 150 ms whereas the decay towards larger latencies is much broader.

Choosing different values of the rate constants for the steps of the chain makes the fit even worse. We also have tried different gainless chain models, but we always failed to make the resulting model

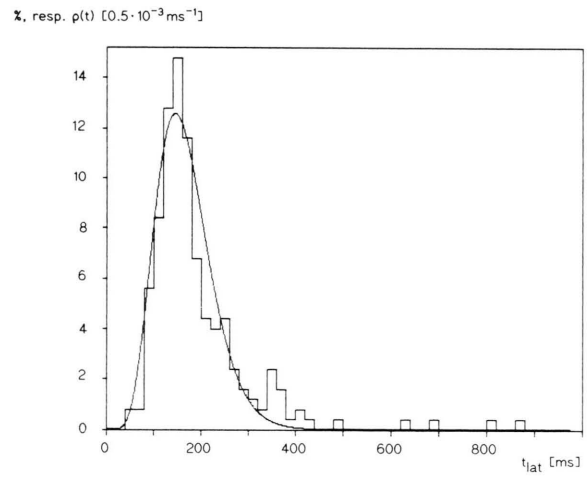

Fig. 4. Fit of $\varrho(t)$ of (4.1) to the experimental histogram of first latencies (see Fig. 2A) with $N = 8$.

density $\varrho(t)$ as well sufficiently sharp as sufficiently asymmetric. For simple chain models, these two aspects seem to exclude each other. This finding caused us to review our approach critically. As a way out of our problem, we suspected that it is crucial for a model description of latency to take into account the statistics of the number of photons delivered by a flash even if its macroscopic intensity remains constant. The number of photons delivered by a flash is Poisson-distributed. If a flash of fixed macroscopic intensity delivers a mean number of $\langle n \rangle$ photons, the probability p_n of having exactly n photons in a particular flash is given by

$$p_n = \frac{\langle n \rangle^n}{n!} e^{-\langle n \rangle} \quad n = 0,1,2,\ldots \tag{4.3}$$

By including the optical absorption constant and the quantum efficiency into the definition of the mean $\langle n \rangle$, we may also interprete $\langle n \rangle$ as the mean number of photons that are captured by rhodopsin molecules per flash and p_n as the probability that exactly n photons are captured by rhodopsin molecules in a particular flash [26].

The inclusion of photon statistics into our analysis has several consequences. Firstly, we note that there is a non-zero probability $p_0 = e^{-\langle n \rangle}$ that no photon is captured. In fact, one observes in bump experiments that a fraction of flashes is not responded by a bump, at least not by a bump above the noise level of the base line.

Obviously, we can determine the mean number $\langle n \rangle$ of photons captured per flash by setting p_0 = fraction of non-responded flashes, such that $\langle n \rangle = -\ln(p_0)$. Secondly, we expect to observe flashes which are responded by two or more bumps which also agrees with the experimental findings, see for example Fig. 1E. The crucial point, however, is that a response to a light flash is recognized as a multi-bump response only if the actual latencies of the component bumps involved in the response are sufficiently different from each other. Obviously, this condition cannot be controlled. If it is not fulfilled we observe the superposition of two or even more bumps and count the response as but one bump (see above). The observed latency of such a superposition event is thus the shortest fpt of two or more latency chains initiated at the same time. We shall argue in the following chapter 5 and 6 that this contest for the shortest fpt makes the

effective latency density typically asymmetric as compared to the density $\varrho(t)$ of a single chain and thus is a step towards a solution of our problem outlined above.

Our conjecture that a finite fraction of responses recorded within the first second after a light flash is a superposition of two or more totally overlapping bumps has still further implications. It means that the experimentally determined histograms of response amplitudes and net charge transfers should be suspected of overestimating the mean values of the bump amplitude and its net charge transfer. In chapter 7, we argue that this effect may give a new answer to the question why the responses recorded immediately after a light flash differ from the so-called spontaneous bumps recorded for larger times (more than about 1 sec after the flash) with respect to the amplitudes and net charge transfers.

5. Latency Densities for First, Second, ... Bumps

In this chapter, we show how to calculate the latency densities of the m − th bump $\varrho_m(t)$ which is defined such that $\varrho_m(t)\mathrm{d}t$ is the probability that the m − th bump response to a flash at $t = 0$ arrives at a time within the interval $(t,t + \mathrm{d}t)$, $m = 1,2,\ldots$ Our starting point is a model chain for the latency process and its single chain fpt-density $\varrho(t)$, a particular example being given by our simple scheme (4.1) with $\varrho(t)$ given by (4.2) in the preceding chapter. For this purpose, we first need an auxiliary expression $\varrho_{m,n}(t)$ defined such that $\varrho_{m,n}(t)\mathrm{d}t$ is the probability that the m − th bump response arrives in $(t,t + \mathrm{d}t)$ after a flash at $t = 0$ which causes the capture of exactly n photons by different rhodopsin molecules. This definition is meant to explicitly include the assumption that the n captured photons initiate different and independent latency chains in the cell which do not interfere with each other. This assumption is satisfied for bump experiments if we assume that the latency process initiated by a photon capture is localized within the microvillus hit by the photon [27] and if we realize that the probability for two or more photons to be absorbed within the same microvillus is vanishingly small since the mean number $\langle n\rangle$ of captured photons per flash turns out to be of the order of $\langle n\rangle \approx 2 \ldots 3$ (*cf.* next chapter) and the number of microvilli per cell is about 10^6 [28]. With these assumptions we can immediately derive $\varrho_m(t)$ from $\varrho_{m,n}(t)$ as

$$\varrho_m(t) = \sum_{n=m}^{\infty} p_n \varrho_{m,n}(t), \tag{5.1}$$

where p_n is again the probability that exactly n photons are captured per flash as expressed in Eqn. (4.3) for given mean number $\langle n\rangle$ of photons captured per flash.

Clearly we have by definition $\varrho_{1,1}(t) = \varrho(t)$. In order to calculate $\varrho_{m,n}(t)$ for arbitrary n and $m \leq n$ we make use of the so-called order statistics [4, 29]. $\varrho_{m,n}(t)\mathrm{d}t$ is the probability that among n bump responses $m - 1$ arrive before t, one arrives in $(t,t + \mathrm{d}t)$ and the remaining $n - m$ arrive after $t + \mathrm{d}t$. Moreover, any permutation of the $m - 1$ bump responses before t and the $n - m$ bump responses after $t + \mathrm{d}t$ yields the same statistical configuration. This consideration leads to

$$\varrho_{m,n}(t)\mathrm{d}t = \frac{n!}{(m-1)!\,(n-m)!}(\Phi(t))^{m-1}(\Phi(t + \mathrm{d}t) - \Phi(t))(1 - \Phi(t))^{n-m} \tag{5.2}$$

where

$$\Phi(t) = \int_0^t \mathrm{d}t'\,\varrho(t') \tag{5.3}$$

is the probability that the bump response of a single latency chain arrives within $(0,t)$. Evaluating the right-hand side of Eqn. (5.2) yields

$$\varrho_{m,n}(t) = \frac{n!}{(m-1)!\,(n-m)!}(\Phi(t))^{m-1}(1 - \Phi(t))^{n-m}\varrho(t). \tag{5.4}$$

Inserting $\varrho_{m,n}(t)$ of Eqn. (5.4) and p_n of Eqn. (4.3) into Eqn. (5.1) and evaluating the n-sum eventually gives

$$\varrho_m(t) = \frac{\langle n\rangle\varrho(t)}{(m-1)!}(\langle n\rangle\Phi(t))^{m-1}\exp(-\langle n\rangle\Phi(t)) \tag{5.5}$$

in particular for the first bump responses ($m = 1$)

$$\varrho_1(t) = \langle n\rangle\varrho(t)\exp(-\langle n\rangle\Phi(t)). \tag{5.6}$$

In the following chapter $\varrho_1(t)$ of Eqn. (5.6) will be used to fit the experimental histogram of the latencies of the first bumps by an appropriate model chain characterized by its fpt-density $\varrho(t)$.

Eqn. (5.6) may also be used to estimate the fpt-density $\varrho(t)$ to be realized by an appropriately chosen single chain model from the experimental

histogram of first bump latencies. To this purpose we derive from Eqn. (5.6) by integrating

$$\Phi_1(t) = \int_0^t \mathrm{d}t' \varrho_1(t') = 1 - \exp(-\langle n \rangle \Phi(t)). \quad (5.7)$$

Inverting the right-hand side of Eqn (5.7) with respect to $\Phi(t)$ gives

$$\Phi(t) = -\frac{1}{\langle n \rangle} \ln(1 - \Phi_1(t)) \quad (5.8)$$

and upon differentiating with respect to t using Eqn. (5.3)

$$\varrho(t) = \frac{1}{\langle n \rangle} \frac{\varrho_1(t)}{1 - \Phi_1(t)}. \quad (5.9)$$

Interpreting $\varrho_1(t)$ as the experimental histogram of first latencies and using an appropriate numerical evaluation method we have estimated the desired shape of the single chain fpt-density $\varrho(t)$ from Eqn. (5.9).

6. Comparison with Experiment

In order to fit the latency density $\varrho_1(t)$ of the first bumps to the experimental histograms we first need an estimate for the mean number $\langle n \rangle$ of photons captured per flash. Let M be the total number of flashes in a particular bump experiment among which M_0 are not responded by a bump such that $p_0 = M_0/M$ is the fraction of non-responded flashes. According to chapter 4 the mean number $\langle n \rangle$ of photons captured per flash is then given as

$$\langle n \rangle = -\ln(p_0) = -\ln(M_0/M). \quad (6.1)$$

Note that the precise meaning of "non-responded flashes" is: non-responded by a detected bump, *i.e.* a bump above the base line noise. Quite formally, the quantum efficiency of the cell might be generalized to include also non-detected bumps such that the number of detected bumps again satisfies a poisson distribution.

Due to the finite number M of flashes the determination of the number M_0 of non-responded flashes is subject to a statistical error. Since the statistical disjunction "response" or "no response" is a two-valued stochastic process we adopt a binomial distribution for the number M_0 of non-responded flashes. As a consequence we expect a statistical error with a variance

$$\sigma^2 = \langle (\Delta M_0)^2 \rangle = M p_0 (1 - p_0) \quad (6.2)$$

for the determination of M_0. This means that the calculation of the mean number $\langle n \rangle$ from Eqn. (6.1) involves a statistical error given by

$$\langle n \rangle_{\min} \leq \langle n \rangle \leq \langle n \rangle_{\max}, \quad (6.3)$$

with

$$\langle n \rangle_{\min} = -\ln\left(\frac{M_0 + \sigma}{M}\right), \langle n \rangle_{\max} = -\ln\left(\frac{M_0 - \sigma}{M}\right). \quad (6.4)$$

For our experiment (KL 98) to which we refer in the following we had a total number of $M = 250$ flashes among which $M_0 = 30$ were unresponded. Inserting these values into Eqns. (6.3) and (6.4) we obtain

$$\langle n \rangle_{\min} = 1.95, \langle n \rangle = 2.12, \langle n \rangle_{\max} = 2.29 \quad (6.5)$$

i.e. a relative error of $\approx 16\%$ which seems acceptable for the following evaluations.

Next we have to choose a model chain and to calculate its fpt-density $\varrho(t)$. Let us begin with our simple model scheme of Eqn. (4.1) and its $\varrho(t)$ given in Eqn. (4.2). In Fig. 5 we show fits of the model density $\varrho_1(t)$ from Eqn. (5.6) to the experimental histogram (KL 98) of the first bump latencies. Let us recall that the rate constant k is determined by the time scale of the experimental histogram (*cf.* chapter 4) whereas the number N of chain steps remains to be used as fit parameter. Fig. 5A shows the fit for $N = 8$, Fig. 5B the one for $N = 10$. The corresponding values of k are 0.038 ms^{-1} and 0.049 ms^{-1} respectively.

The fit in Fig. 5 is improved as compared to that of Fig. 4 with the bare fpt-density $\varrho(t)$, *i.e.*, without renormalization by photon statistics. This confirms our statement that photon statistics has to be taken into account when evaluating experimental latency histograms and drawing conclusions therefrom for the molecular mechanisms of photoreception. Nevertheless, there are still shortcomings of the fit in Fig. 5. First of all, the fact that our best fit is obtained for a number of $N = 8$ steps of the latency chain puts the question whether this figure is plausible in view of a biochemical consideration. Secondly, even the fit with $N = 8$ is not quite satisfactory: although the model density $\varrho_1(t)$ describes the experimental latency times almost perfectly for times t smaller than 150 ms it deviates from the experimental histograms for larger times, partly overestimating and partly underestimating them. This deviation may partly be caused by the statisti-

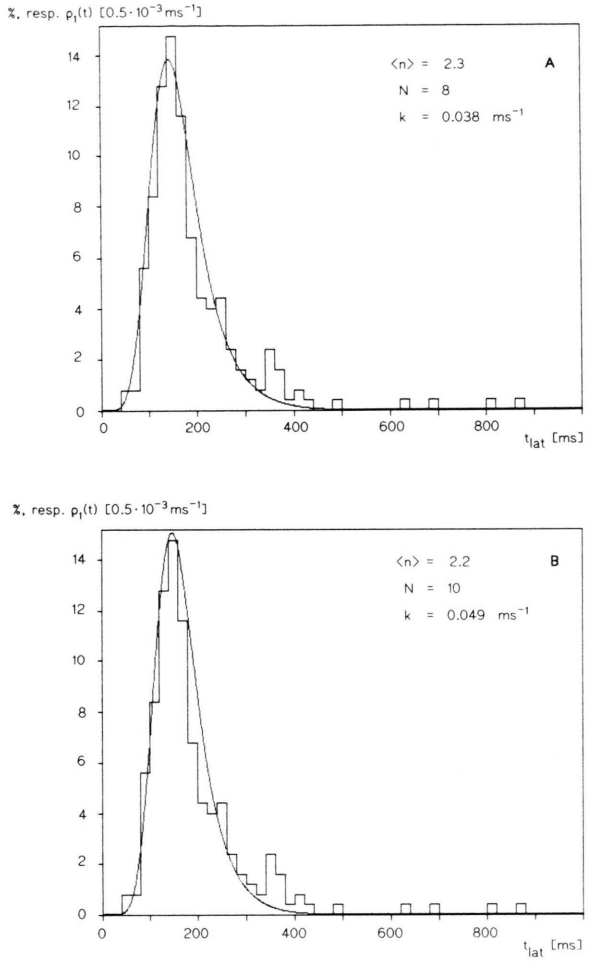

Fig. 5. Fits of the latency density $\varrho_1(t)$ of first bumps as calculated from the chain model of Eqn. (4.1) to the experimental histogram for $N = 8$ (A) and $N = 10$ (B) model chain steps. The values of N, k used in Eqn. (4.2) and the value of $\langle n \rangle$ used within Eqn. (5.6) are indicated in the figures.

cal errors due to the finite number of flashes, but apart from that it is also due to the fact that the single chain fpt-density $\varrho(t)$ of our simple model is much too stiff: any change of the number N of steps implies a change of the complete time scale. We have therefore tried another chain model which is schematically shown in Eqn. (6.6):

$$\begin{aligned} &\text{photon capture} \rightarrow M^* \rightarrow M^0 \\ &\qquad A + M^* \rightarrow K + M^* \qquad (6.6) \\ &X_0 + K \rightarrow X_1 + K, X_1 + K \rightarrow X_2 + K, \ldots, \\ &X_{N-1} + K \rightarrow X_N + K. \end{aligned}$$

M* is the active conformation of metarhodopsin which decays into an inactive conformation M^0. While M* is active it is assumed to form catalysts K from a reservoir A of precessors. The catalysts K are assumed to cause N conformational changes of a molecule X_0 step by step until eventually the conformation X_N starts amplification. The third line of our scheme (6.6) is similar to the simple chain scheme of Eqn. (4.1), however, the transition rates of the conformational steps of the X-molecules now depend on the number of catalysts K which is time-dependent. This makes the time behaviour completely different from that of the scheme of Eqn. (4.1) such that now a number of only $N = 3$ conformational changes turns out to be sufficient for a realistic description of the latency histogram. We do not go into any mathematical details of the model. Fig. 6 shows our best fit with $N = 3$ and appropriately chosen rate constants for the reactions contained in the scheme (6.6).

In order to discuss further implications of our approach, we return to our simple chain model of Eqn. (4.1). Figure 7 shows a comparison of its single chain fpt-density $\varrho(t)$ given by Eqn. (4.2) with the corresponding model latency time densities of the m − th bumps, $\varrho_m(t)$, for $m = 1,2,3,4$. First of all we see that the $\varrho_m(t)$ become skewed towards shorter latencies as compared to $\varrho(t)$, in particular that for $m = 1$. This is exactly how the experimental latency histograms differ from model fpt-distri-

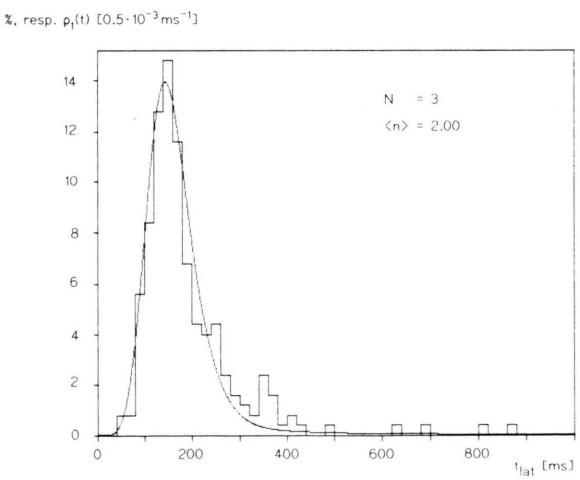

Fig. 6. Fit of the latency time density $\varrho_1(t)$ of first bumps as calculated from the model scheme of Eqn. (6.6) to the experimental histogram (compare Fig. 2A).

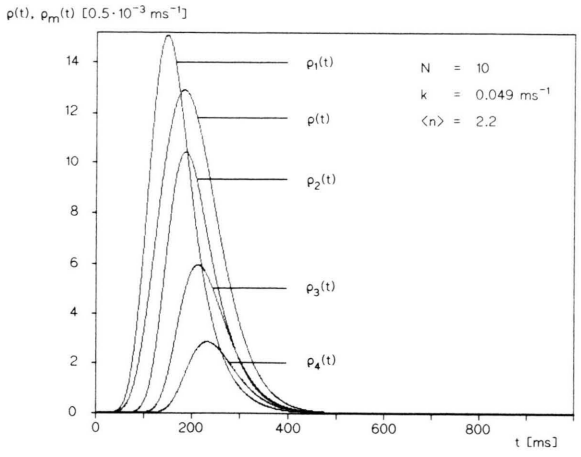

Fig. 7. Comparison of the single chain fpt-time density $\varrho(t)$ of the model scheme of Eqn. (4.1) with the corresponding m − th bump latency time densities $\varrho_m(t)$. Parameter values for the model chain and $\langle n \rangle$ are indicated in the figure.

butions which tend to be symmetric without renormalization by photon statistics. The skewing towards shorter latencies is a consequence of our assumption that the experimentally observed latency is always the shortest fpt of a number of more than one independent transduction chains if the light flash has caused the successful capture of more than one photon. Secondly, we observe a broad overlap of the latency time densities $\varrho_m(t)$ of the m − th bumps for different values of m. As a consequence, we have to visualize that due to a time overlap a considerable portion of second, third, ... bumps will not be recognized as such when evaluating bump experiments. As pointed out already in chapter 4, this means that a considerable portion of up to 20% (estimated from our data) of totally overlapping response events will be mistaken as single bumps which in turn causes an overestimation of the amplitudes and net charge transfers of quantum bumps. We shall discuss this hypothesis in the following chapter.

7. Simulation of Bump Superposition

As pointed out already in chapter 3, the mean values of parameters amplitude, net charge transfer and response duration of the bumps recorded within about 1 sec after the light flash turn out to be recognizably larger than those of the bumps recorded at later times, the so-called spontaneous bumps (*cf.* Fig. 3). Lamb [6] and Lisman [7] have conjectured that the spontaneous bumps are caused by a molecular mechanism different from that of the light-evoked bumps, namely by a spontaneous backward reaction of inactivated rhodopsin into an active configuration. This conjecture necessarily involves a specific assumption: in order to account for the different sizes of the spontaneous bumps, the active rhodopsin configuration produced by the spontaneous backward reaction and the transduction pathway leading from the backward configuration to the opening of channels have to be different from that of the light-evoked bumps.

Our hypothesis to be presented in this chapter is that light-evoked and spontaneous bumps are caused by the same rhodopsin configuration which is produced either by direct photoisomerization or by a spontaneous backward reaction and take the same pathway up to the opening of channels. We shall argue that the difference in the size of the responses can simply be ascribed to the superposition of bump responses immediately after the light flash. In order to substantiate our hypothesis we have performed a computer simulation of bump superposition by the following steps:

(1) Choice of a particular bump experiment (KL 98 in our case), determination of the mean number $\langle n \rangle$ of photon captures per flash, evaluation of the histograms of latency time, amplitude, net charge transfer and response duration of the bump responses before a time $T_0 = 1000$ ms after the light flash.

(2) Evaluation of amplitudes, net charge transfers and response durations of bump responses later than T_0. These values are stored in a list.

(3) Choice of a latency model (model scheme of Eqn. (6.6) in our case) which is fitted to the experiment chosen in (1). With given value of $\langle n \rangle$, we can calculate the latency densities $\varrho_{m,n}(t)$ from the model, *i.e.*, the probability density of the latency time of the m − th bump response after a light flash at $t = 0$ which causes the capture of exactly n photons (*cf.* chapter 5).

(4) Simulation of light flashes: we first choose the number of photons n to be captured in a particular flash by realizing random numbers n which satisfy the Poisson distribution of Eqn. (4.3) for given value of $\langle n \rangle$. For given number n of cap-

tured photons and hence of n single bump responses to be simulated we then choose the time instants of the responses by realizing random times which satisfy the densities $\varrho_{m,n}(t)$. Next, n bumps of the list of measured responses after T_0 are chosen at random (*cf.* (2)) and superposed according to the latency times determined before. This superposition is done numerically on the computer by using an appropriate spline function into which the bump parameters of the list are inserted.

(5) Finally, the numerically superimposed response consisting of experimentally observed bump individuals is analyzed with respect to the bump parameters amplitude, net charge transfer and response duration in the same way as for the measured bump responses before T_0, *cf.* (1) above.

Steps (4) and (5) are performed M times where M is the total number of flashes in the experiment to which we refer (M = 250 for KL 98 in our case). Fig. 8 shows a comparison of the histograms for amplitude and net charge transfer resulting from the simulation procedure with those of the original response events before T.

Comparing the histograms of simulated superpositions in Fig. 8 with the histograms of bumps recorded after T_0 in Fig. 3 one recognizes that the superposition of bumps shifts the histograms of amplitudes and net charge transfers towards larger values, as expected. The histogram of the amplitudes of simulated light-evoked responses before T_0 in Fig. 8 A agrees with that of measured responses before T_0 at least qualitatively, for the net charge transfers in Fig. 8 B the agreement is almost quantitative. The histograms of the response duration of simulated and measured light-evoked responses also show an almost quantitative agreement.

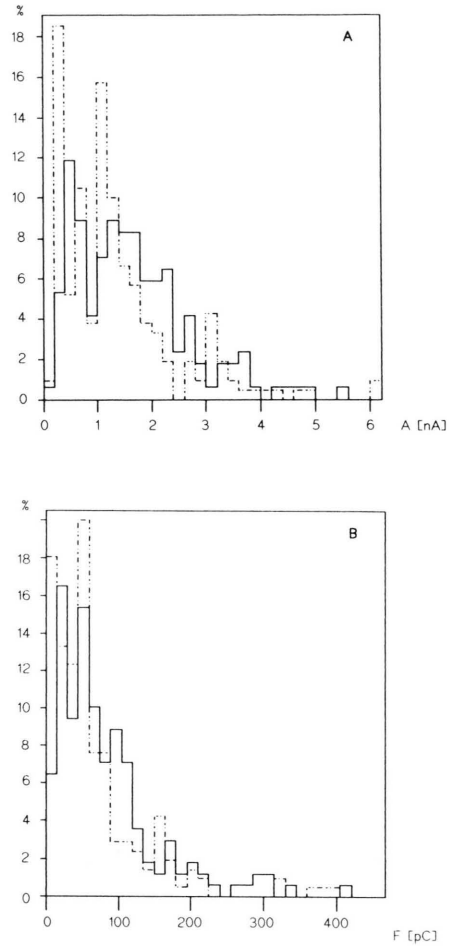

Fig. 8. Histograms of amplitudes (A) and net charge transfers (B) of simulated response events (dotted line, 210 events) and measured response events (full line, 169 events) before T_0.

Our conclusion from the results of our simulation shown in Fig. 8 is that the assumption of different initiation steps and transduction pathways for light-evoked and spontaneous bumps (after T_0) is not compelling. Both the light-evoked bumps (before T_0) and the spontaneous bumps (after T_0) may be caused by the same rhodopsin configuration along the same transduction pathway.

8. Conclusion

In quantum bump experiments using light flashes as the stimulus, a light flash of constant intensity may release fluctuating numbers $n = 0,1,2,\ldots$ of photons due to the Poisson statistics of photons. Assuming a constant quantum efficiency per photon, the numbers n of bump responses per flash will also obey a Poisson distribution with some mean value $\langle n \rangle$ which can be evaluated from the portion of non-responded flashes. We have shown that the Poisson statistics of bump responses has to be taken into account when evaluating the experimental results and drawing conclusions from them since otherwise the distinctly skewed experimental histograms of latencies can hardly be understood on the basis of a chemical transduc-

tion model. The main effect of the Poisson statistics of the responses evoked by a single flash is the fact that responses due to the capture of more than one photon per flash may more or less overlap as functions of time and that for flashes evoking a number of 2 to 3 bumps on the average a fraction of up to 20% is expected to overlap almost completely such that they will not be recognized as different responses.

We have discussed some implications of the response statistics in flash experiments. Firstly, the experimentally obtained histogram of bump latencies cannot be expected to represent the bare first passage time histogram of one-photon events in the underlying chemical latency mechanism. We have shown how the first passage time distribution of one-photon events can be recalculated from the experimental histogram of bump responses if the mean number $\langle n \rangle$ of bumps per flash is known. Or *vice versa:* if one starts with a chemical latency model and calculates its first passage time distribution for one-photon events, the latency histogram to be observed in an experiment is expected to be skewed towards shorter latencies since the latencies of second, third, ... responses of the same flash cannot be detected if the overlapping is almost complete. Extrapolating this statistical effect to high values of flash intensities giving rise to macroscopic responses, one may predict how the latency of arbitrary responses should decrease as a function of the intensity of the stimulus flash. One of us (R. L. [4]) has worked out this idea and obtained quite a satisfying agreement with the experimental results.

A second implication of the response statistics in flash experiments is the fact that due to the overlapping of the one-photon responses evoked by a flash the size (amplitude, net charge transfer) of flash responses is expected to be overestimated as compared to that of true one-photon responses. We have argued that this may explain why flash-evoked bump responses are found to be larger in size as compared to the so-called spontaneous bumps recorded at times larger than about 1 s after the flash. We have confirmed this idea by a numerical simulation of flash responses using the experimentally recorded spontaneous bumps as simulation material for true one-photon responses and found satisfying agreement with the experimental results. On these grounds and adopting Lamb's and Lisman's hypothesis that spontaneous bumps are caused by spontaneous backward reactions of inactivated rhodopsin into an active configuration, we suggest that light-evoked and spontaneous bumps start from the same activated rhodopsin state and take the same biochemical transduction pathway. As a consequence we would expect that for sufficiently weak flashes light-evoked and spontaneous bumps will no longer differ with respect to their amplitudes and net charge transfers.

[1] H. Stieve, in: The Molecular Mechanism of Photoreception (H. Stieve, ed.), Dahlem-Konferenz, pp. 199–230, Springer Verlag, Berlin, Heidelberg, New York 1986.
[2] J. Schnakenberg, Biol. Cybern. **60,** 421–437 (1989).
[3] M. G. F. Fuortes and A. L. Hodgkin, J. Physiol. **172,** 239–263 (1964).
[4] R. Lederhofer, Thesis, RWTH Aachen, F.R.G. 1989.
[5] R. Payne and A. Fein, J. Gen. Physiol. **87,** 243–296 (1986).
[6] T. D. Lamb, Vision Res. **21,** 1773–1782 (1981).
[7] J. Lisman, J. Gen. Physiol. **70,** 171–187 (1985).
[8] H. Stieve, M. Pflaum, J. Klomfaß, and H. Gaube, Z. Naturforsch. **40c,** 278–294 (1985).
[9] H. Stieve, H. Reuß, T. Hennig, and J. Klomfaß, in preparation (1990).
[10] H. Stieve and M. Bruns, Biophys. Struct. Mech. **6,** 271–285 (1980).
[11] H. Stieve and M. Bruns, Biophys. Struct. Mech. **9,** 329–339 (1983).
[12] A. R. Adolph, J. Gen. Physiol. **52,** 584–599 (1968).
[13] R. Srebo and M. Behbehani, J. Physiol. **224,** 349–361 (1972).
[14] F. Wong, Nature **276,** 76–79 (1978).
[15] J. Bacigalupo and J. E. Lisman, Nature **304,** 268–270 (1983).
[16] J. Bacigalupo and J. E. Lisman, Biophys. Journal **45,** 3–5 (1984).
[17] K. Nagy and H. Stieve, Europ. Biophys. J., in press (1990).
[18] F. Wong, B. W. Knight, and F. A. Dodge, J. Gen. Physiol. **76,** 517–537 (1980).
[19] J. Howard, Biophys. Struct. Mech. **9,** 341–348 (1983).
[20] W. Keiper, Thesis, RWTH Aachen, F.R.G. 1983.
[21] W. Keiper, J. Schnakenberg, and H. Stieve, Z. Naturforsch. **39c,** 781–790 (1984).
[22] A. Borsellino and M. G. F. Fuortes, J. Physiol. **196,** 507–539 (1968).
[23] D. A. Baylor, A. L. Hodgkin and T. D. Lamb, J. Physiol. **242,** 685–727 (1974).
[24] J. Schnakenberg and W. Keiper, in: The Molecular Mechanism of Photoreception (H. Stieve, ed.), Dahlem-Konferenz, pp. 353–367, Springer Verlag, Berlin, Heidelberg, New York 1986.
[25] N. G. van Kampen, Stochastic Processes in Physics and Chemistry, p. 174, North-Holland Publishing, Amsterdam, New York, Oxford 1981.
[26] K. Kirschfeld, in: The Functional Organization of the Compound Eye (C. G. Bernhard, ed.), p. 302, Pergamon Press 1966.
[27] U. W. Becker, N. H. Nuske, and H. Stieve, in: Progress in Retinal Research (N. Osborne and J. Chader, eds.), **Vol. 8,** pp. 229–253, Pergamon Press 1988.
[28] G. B. Calman and S. C. Chamberlain, J. Gen. Physiol. **80,** 839–862 (1982).
[29] H. A. David, Order Statistics, Wiley, New York 1970.